Learning Multiple Networks via Supervised Tensor Decomposition

Jiaxin Hu
Department of Statistics
University of Wisconsin-Madison
Madison, WI 53706
jhu267@wisc.edu

Chanwoo Lee
Department of Statistics
University of Wisconsin-Madison
Madison, WI 53706
chanwoo.lee@wisc.edu

Miaoyan Wang
Department of Statistics
University of Wisconsin-Madison
Madison, WI 53706
miaoyan.wang@wisc.edu

Abstract

We consider the problem of tensor decomposition with multiple side information available as interactive features. Such problems are common in neuroimaging, network modeling, and spatial-temporal analysis. We develop a new family of exponential tensor decomposition models and establish the theoretical accuracy guarantees. An efficient alternating optimization algorithm is further developed. Unlike earlier methods, our proposal is able to handle a broad range of data types, including continuous, count, and binary observations. We apply the method to diffusion tensor imaging data from human connectome project and identify the key brain connectivity patterns associated with available features. Our method will help the practitioners efficiently analyze tensor datasets in various areas. Toward this end, all data and code are available at `https://CRAN.R-project.org/package=tensorregress`.

1 Introduction

Higher-order tensors have received increased attention across science and engineering. While most tensor decomposition methods are developed for a single tensor observation, scientific studies often collect side information, in the form of node features and interactions thereof, together with the tensor data. Such data problems are common in neuroimaging, network analysis, and spatial-temporal modeling. A popular example is in neuroimaging (Zhou et al., 2013). The brain connectivity networks are collected from a sample of individuals, accompanied by individual characteristics such as age, gender, and diseases status (see Figure 1a). Another example is in network analysis (Berthet and Baldin, 2020). Side information such as people's demographic information and friendship types are often available. In both examples, scientists are interested in identifing the variation in the data tensor (e.g., brain connectivities, social community patterns) that is affected by available features. These seemingly different scenarios pose a common yet challenging problem for tensor data modeling.

In addition to the challenge of incorporating side information, another challenge is that many tensor datasets consist of non-Gaussian measurements (Wang and Li, 2020; Lee and Wang, 2020) . Classical tensor decomposition methods are based on minimizing the Frobenius norm of deviation, leading to suboptimal predictions for binary- or count-valued response variables. A number of supervised tensor methods have been proposed (Narita et al., 2012; Zhao et al., 2012; Yu and Liu, 2016; Lock and Li, 2018). These methods often assume Gaussian distribution for the tensor entries, or impose random designs for the feature matrices, both of which are less suitable for applications of our interest.

Third Workshop on Machine Learning and the Physical Sciences (NeurIPS 2020), Vancouver, Canada.

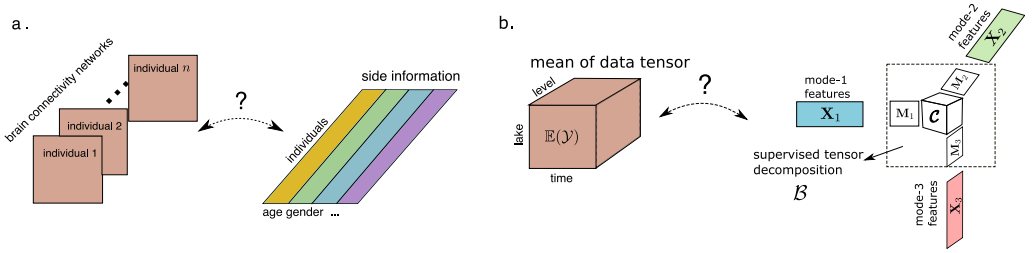

Figure 1: Examples of supervised tensor decomposition with interactive side information. (a) Network population model. (b) Spatio-temporal growth model.

Our contribution. This paper presents a general model and associated method for decomposing a data tensor whose entries are from exponential family with interactive side information. We formulate the learning task as a low-rank tensor regression problem, with tensor observation serving as the response, and the multiple side information as interactive features. We blend the modeling power of generalized linear model (GLM) and the exploratory capability of tensor dimension reduction in order to take the best out of both sides. Our method greatly improves the classical tensor decomposition, and we quantify the improvement in prediction through numerical experiments and data applications.

Notation. We follow the tensor notation as in Kolda and Bader (2009). The multilinear multiplication of a tensor $\mathcal{Y} \in \mathbb{R}^{d_1 \times \cdots \times d_K}$ by matrices $\boldsymbol{X}_k = [\![x^{(k)}_{i_k,j_k}]\!] \in \mathbb{R}^{p_k \times d_k}$ is defined as $\mathcal{Y} \times \{\boldsymbol{X}_1, \ldots, \boldsymbol{X}_K\} = [\![\sum_{i_1,\ldots,i_K} y_{i_1,\ldots,i_K} x^{(1)}_{j_1,i_1} \cdots x^{(K)}_{j_K,i_K}]\!]$, which results in an order-K $(p_1, \ldots, p_K)$-dimensional tensor. The inner product between two tensors of equal size is defined as $\langle \mathcal{Y}, \mathcal{Y}' \rangle = \sum_{i_1,\ldots,i_K} y_{i_1,\ldots,i_K} y'_{i_1,\ldots,i_K}$. We use $\|\cdot\|_F$ and $\|\cdot\|_\infty$ to denote tensor F-norm and tensor infinity norm, respectively. We use $\mathrm{vec}(\cdot)$ to denote the operation that reshapes the tensor into a vector, and $\mathrm{Unfold}_k(\cdot)$ to denote the operation that reshapes the tensor along mode k into a matrix of size d_k-by-$\prod_{i \neq k} d_i$. We also use $\|\cdot\|_\sigma$ and $\otimes$ to denote the matrix spectral norm and Kronecker product of matrices, respectively. For ease of notation, we allow basic arithmetic operators (e.g., $+, -$) and univariate functions $f\colon \mathbb{R} \to \mathbb{R}$ to be applied to tensors in an element-wise manner.

2 Proposed models and motivating examples

Let $\mathcal{Y} = [\![y_{i_1,\ldots,i_K}]\!] \in \mathbb{R}^{d_1 \times \cdots \times d_K}$ denote an order-K data tensor. Suppose the side information is available on each of the K modes. Let $\boldsymbol{X}_k = [\![x_{ij}]\!] \in \mathbb{R}^{d_k \times p_k}$ denote the feature matrix on the mode $k \in [K]$, where x_{ij} denotes the j-th feature value for the i-th tensor entity, for $(i, j) \in [d_k] \times [p_k]$, $p_k \leq d_k$. We assume that, conditional on the features $\boldsymbol{X}_k$, the entries of tensor $\mathcal{Y}$ are independent realizations from an exponential family distribution, and the conditional mean tensor admits the form

$$\mathbb{E}(\mathcal{Y} | \boldsymbol{X}_1, \ldots, \boldsymbol{X}_K) = f\left(\mathcal{C} \times \{\boldsymbol{X}_1 \boldsymbol{M}_1, \ldots, \boldsymbol{X}_K \boldsymbol{M}_K\}\right), \quad \text{with } \boldsymbol{M}_k^T \boldsymbol{M}_k = \boldsymbol{I}_{r_k},\ \boldsymbol{M}_k \in \mathbb{R}^{p_k \times r_k} \quad \text{for all } k = 1, \ldots, K. \tag{1}$$

where $\mathcal{C} \in \mathbb{R}^{r_1 \times \cdots \times r_K}$ is a full-rank core tensor, $\boldsymbol{M}_k \in \mathbb{R}^{p_k \times r_k}$ are factor matrices consisting of orthonormal columns with $r_k \leq p_k$ for all $k \in [K]$, and $f(\cdot)$ is a known link function whose form depending on the data type of $\mathcal{Y}$. Common choices of link functions include identity link for Gaussian distribution, logistic link for Bernoulli distribution, and $\exp(\cdot)$ link for Poisson distribution.

Figure 1b provides a schematic illustration of our model. The features $\boldsymbol{X}_k$ affect the distribution of tensor entries in $\mathcal{Y}$ through the sufficient features of the form $\boldsymbol{X}_k \boldsymbol{M}_k$, which are r_k linear combinations of features on mode k. The core tensor $\mathcal{C}$ collects the interaction effects between sufficient features across K modes, and thus allows the identification of variations in the tensor data attributable to the side information. Our goal is to find $\boldsymbol{M}_k$ and the corresponding $\mathcal{C}$ to reveal the relationship between side information $\boldsymbol{X}_k$ and the observed tensor $\mathcal{Y}$. Note that $\boldsymbol{M}_k$ and $\mathcal{C}$ are identifiable only up to orthonormal transformations.

We give two examples of supervised tensor decomposition models (1) that arise in practice.

Example 1 (Spatio-temporal growth model)**.** The growth curve model (Srivastava et al., 2008) was originally proposed as an example of bilinear model for matrix data, and we extend it to higher-order cases. Let $\mathcal{Y} = [\![y_{ijk}]\!] \in \mathbb{R}^{d \times m \times n}$ denote the pH measurements of d lakes at m levels of depth and for n time points. Suppose the sampled lakes belong to q types, with p lakes in each type. Let $\{\ell_j\}_{j \in [m]}$ denote the sampled depth levels and $\{t_k\}_{k \in [n]}$ the time points. Assume that the expected

pH trend in depth is a polynomial of order at most r and that the expected trend in time is a polynomial of order s. Then, the conditional mean model for the spatio-temporal growth is a special case of our model (1), where $\boldsymbol{X}_1 = \text{blockdiag}\{\mathbf{1}_q, \ldots, \mathbf{1}_q\} \in \{0,1\}^{d \times p}$ is the design matrix for lake types,

$$\boldsymbol{X}_2 = \begin{pmatrix} 1 & \ell_1 & \cdots & \ell_1^r \\ 1 & \ell_2 & \cdots & \ell_2^r \\ \vdots & \vdots & \ddots & \vdots \\ 1 & \ell_m & \cdots & \ell_m^r \end{pmatrix}, \; \boldsymbol{X}_3 = \begin{pmatrix} 1 & t_1 & \cdots & t_1^s \\ 1 & t_2 & \cdots & t_2^s \\ \vdots & \vdots & \ddots & \vdots \\ 1 & t_n & \cdots & t_n^s \end{pmatrix}$$

are the design matrices for spatial and temporal effects, respectively. The spatial-temporal mode has covariates available on each of the three modes.

Example 2 (Network population model)**.** Network response model is recently developed in the context of neuroimanig analysis. The goal is to study the relationship between network-valued response and the individual covariates. Suppose we observe n i.i.d. observations $\{(\boldsymbol{Y}_i, \boldsymbol{x}_i) : i = 1, \ldots, n\}$, where $\boldsymbol{Y}_i \in \{0,1\}^{d \times d}$ is the brain connectivity network on the i-th individual, and $\boldsymbol{x}_i \in \mathbb{R}^p$ is the individual covariate such as age, gender, cognition, etc. The network-response model (Rabusseau and Kadri, 2016) has the form

$$\text{logit}(\mathbb{E}(\boldsymbol{Y}_i | \boldsymbol{x}_i)) = \mathcal{B} \times_3 \boldsymbol{x}_i, \quad \text{for } i = 1, \ldots, n \tag{2}$$

where $\mathcal{B} \in \mathbb{R}^{d \times d \times p}$ is the coefficient tensor of interest, and $\times_3$ denotes the tensor-by-matrix multiplication along the 3rd mode (Kolda and Bader, 2009). The model (2) is also a special case of our tensor-response model, with covariates on the last mode of the tensor.

3 Estimation methods with accuracy guarantees

We develop a likelihood-based procedure to estimate $\mathcal{C}$ and $\boldsymbol{M}_k$ in (1). Ignoring constants that do not depend on Θ, the quasi log-likelihood of (1) is equal to

$$\mathcal{L}_{\mathcal{Y}}(\mathcal{C}, \boldsymbol{M}_1, \ldots, \boldsymbol{M}_K) = \langle \mathcal{Y}, \Theta \rangle - \sum\nolimits_{i_1, \ldots, i_K} b(\theta_{i_1, \ldots, i_K}) \text{ with } \Theta = \mathcal{C} \times \{\boldsymbol{M}_1 \boldsymbol{X}_1, \ldots, \boldsymbol{M}_K \boldsymbol{X}_K\},$$

where $b(\theta) = \theta^2/2$ for Gaussian response, $b(\theta) = \exp(\theta)$ for Poisson response, and $b(\theta) = \log(1 + \exp(\theta))$ for Bernoulli response. We propose a constrained maximum quasi-likelihood estimator (M-estimator),

$$(\hat{\mathcal{C}}, \hat{\boldsymbol{M}}_1, \ldots, \hat{\boldsymbol{M}}_k) = \underset{(\mathcal{C}, \boldsymbol{M}_1, \ldots, \boldsymbol{M}_K) \in \mathcal{P}}{\arg\max} \; \mathcal{L}_{\mathcal{Y}}(\mathcal{C}, \boldsymbol{M}_1, \ldots, \boldsymbol{M}_K), \tag{3}$$

where parameter space $\mathcal{P} = \Big\{ (\mathcal{C}, \boldsymbol{M}_1, \ldots, \boldsymbol{M}_K) \;\Big|\; \boldsymbol{M}_k^T \boldsymbol{M}_k = \mathbf{I}_{r_k}, \; \|\Theta(\mathcal{C}, \boldsymbol{M}_1, \ldots, \boldsymbol{M}_K)\|_\infty \le \alpha \Big\}$, and α is a constant. The maximum norm constraint on the linear predictor Θ is a technical condition to avoid the divergence of the non-Gaussian variance.

The decision variables in the objective function (3) consist of $K+1$ blocks of variables, one for the core tensor $\mathcal{C}$ and K for the factor matrices $\boldsymbol{M}_k$. We notice that, if any K out of the $K+1$ blocks of variables are known, then the optimization reduces to a simple GLM with respect to the last block of variables. This observation leads to an iterative updating scheme for one block at a time while keeping others fixed. A simplified version of the algorithm is described in Algorithm 1.

We provide the accuracy guarantee for the proposed M-estimator (3) by leveraging recent development in random tensor theory and high-dimensional statistics.

Theorem 3.1 (Statistical Convergence)**.** Let $(\hat{\mathcal{C}}, \hat{\boldsymbol{M}}_1, \ldots, \hat{\boldsymbol{M}}_K)$ be the M-estimator in (3) and $\hat{\mathcal{B}} = \hat{\mathcal{C}} \times \{\hat{\boldsymbol{M}}_1, \cdots, \hat{\boldsymbol{M}}_K\}$. Define $r_{\text{total}} = \prod_k r_k$, $r_{\max} = \max_k r_k$, and $\mathcal{B}_{\text{true}} = \mathcal{C} \times \{\boldsymbol{M}_1, \cdots, \boldsymbol{M}_K\}$. Under mild technical assumptions, there exist two positive constants $C_1, C_2 > 0$, such that, with probability at least $1 - \exp(-C_1 \sum_k p_k)$,

$$\|\mathcal{B}_{\text{true}} - \hat{\mathcal{B}}\|_F^2 \le \frac{C_2 r_{\text{total}}}{r_{\max}} \frac{\sum_k p_k}{\prod_k d_k}, \quad \text{and} \quad \sin^2 \Theta(\boldsymbol{M}_{k,\text{true}}, \hat{\boldsymbol{M}}_k) \le \frac{C_2 r_{\text{total}}}{r_{\max} \sigma_{\min}^2(\text{Unfold}_k(\mathcal{C}_{\text{true}}))} \frac{\sum_k p_k}{\prod_k d_k},$$

where $\sin \Theta(\boldsymbol{M}_{k,\text{true}}, \hat{\boldsymbol{M}}_k) = \|\boldsymbol{M}_{k,\text{true}}^T \hat{\boldsymbol{M}}_k^\perp\|_\sigma$ is the angle distance between column spaces.

Theorem 3.1 implies that the estimation has a convergence rate $\mathcal{O}(d^{-(K-1)})$ in the special case when tensor dimensions are equal on every mode, i.e., $d_k = d$ for all $k \in [K]$, and feature dimension grows with tensor dimension, $p_k = \gamma d$, $\gamma \in [0, 1)$, for $k \in [K]$. The convergence of our estimation becomes favorable as the order of tensor data increases. The proof is provided in the Xu et al. (2019).

Algorithm 1 Supervised Tensor Decomposition with Interactive Side Information

Input: Response tensor $\mathcal{Y} \in \mathbb{R}^{d_1 \times \cdots \times d_K}$, feature matrices $\boldsymbol{X}_k \in \mathbb{R}^{d_k \times p_k}$ for $k = 1, \ldots, K$, target Tucker rank $\boldsymbol{r} = (r_1, \ldots, r_K)$, link function f, maximum norm bound α

Output: Estimated core tensor $\hat{\mathcal{C}} \in \mathbb{R}^{r_1 \times \cdots \times r_K}$ and factor matrices $\hat{\boldsymbol{M}}_k \in \mathbb{R}^{p_k \times r_k}$.

1: Random initialization of the core tensor $\mathcal{C}$ and factor matrices $\boldsymbol{M}_k$.
2: **while** Do until convergence **do**
3: **for** $k = 1$ to K **do**
4: Obtain the factor matrix $\tilde{\boldsymbol{M}}_k \in \mathbb{R}^{p_k \times r_k}$ by a GLM with link function f.
5: Perform QR factorization $\tilde{\boldsymbol{M}}_k = \boldsymbol{Q}\boldsymbol{R}$. Update $\boldsymbol{M}_k \leftarrow \boldsymbol{Q}$ and core tensor $\mathcal{C} \leftarrow \mathcal{C} \times_k \boldsymbol{R}$.
6: **end for**
7: Update the core tensor $\mathcal{C}$ by solving a GLM with $\mathrm{vec}(\mathcal{Y})$ as response, $\otimes_{k=1}^{K}[\boldsymbol{X}_k \boldsymbol{M}_k]$ as features, with link function f. Rescale the core tensor $\mathcal{C}$ such that $\|\Theta(\mathcal{C}, \boldsymbol{M}_1, \ldots, \boldsymbol{M}_K)\|_\infty \leq \alpha$.
8: **end while**

4 Numerical experiments

We evaluate the empirical performance of our supervised tensor decomposition (**STD**) through simulations. We consider order-3 tensors, where the conditional mean tensor is generated form model (1). Given the generated linear predictor $\Theta = [\![\theta_{ijk}]\!] = \mathcal{C} \times \{\boldsymbol{M}_1\boldsymbol{X}_1, \boldsymbol{M}_2\boldsymbol{X}_3, \boldsymbol{M}_3\boldsymbol{X}_3\}$, the entries in the tensor $\mathcal{Y} = [\![y_{ijk}]\!]$ are drawn independently according to three probabilistic models: (a) Gaussian model: $y_{ijk} \sim N(\theta_{ijk}, 1)$; (b) Poisson model: $y_{ijk} \sim \text{Poisson}\left(e^{\theta_{ijk}}\right)$; (c) Bernoulli model: $y_{ijk} \sim \text{Bernoulli}\left(e^{\theta_{ijk}}/1 + e^{\theta_{ijk}}\right)$.

The experiment I evaluates the accuracy when covariates are available on all modes. We set $\alpha = 10, d_k = d, p_k = 0.4d_k, r_k = r \in \{2, 4, 6\}$ and increase d from 25 to 50. Our theoretical analysis suggests that $\hat{\mathcal{B}} = \hat{\mathcal{C}} \times \{\hat{\boldsymbol{M}}_1, \hat{\boldsymbol{M}}_2, \hat{\boldsymbol{M}}_3\}$ has a convergence rate $\mathcal{O}(d^{-2})$ in this setting. Figure 2a plots the estimation error versus the effective sample size (d^2), under three different distribution models. We found that the empirical mean squared error (MSE) decreases roughly at the rate of $1/d^2$, which is consistent with our theoretical ascertainment. Similar behaviors can be observed in the non-Gaussian data in Figure 2b-c.

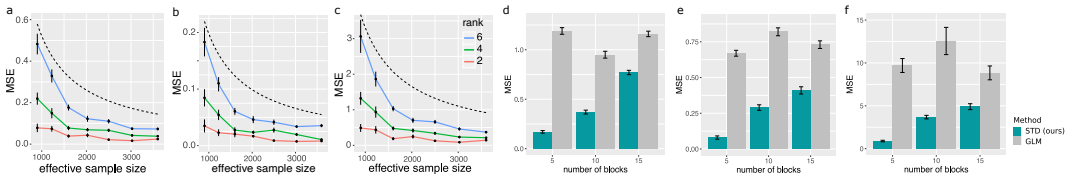

Figure 2: (a)-(c): Estimation error against effective sample size. The dashed curves correspond to $\mathcal{O}(1/d^2)$. (d)-(f): Performance comparison under stochastic block models. The x-axis represents the number of blocks in the networks. Response tensors are generated from Gaussian (a, d), Poisson (b, e) and Bernoulli (d, f) models .

The experiment II investigates the capability of our model in handling correlation among coefficients. We mimic the scenario of brain imaging analysis. A sample of $d_3 = 50$ networks are simulated, where each network measures the connections between $d_1 = d_2 = 20$ brain nodes. We simulate $p = 5$ features for the each of the 50 individuals. These features may represent, for example, age, gender, cognitive score, etc. Recent study has suggested that brain connectivity networks often exhibit community structure represented as a collection of subnetworks, and each subnetwork is comprised of a set of spatially distributed brain nodes. To accommodate this structure, we utilize the stochastic block model (Abbe, 2017) to generate the effect size. Specifically, we partition the nodes into r blocks by assigning each node to a block with uniform probability. Edges within a same block are assumed to share the same feature effects, where the effects are drawn i.i.d. from $N(0, 1)$.

Figure 2d-f compares the MSE of our method with a multiple-response GLM approach. The multiple-response GLM is to regress the dyadic edges, one at a time, on the features, and this model is repeatedly fitted for each edge. As we find in Figure 2d-f, our tensor regression method achieves significant error reduction in all three data types considered. The outperformance is substantial in the presence of large communities; even in the less structured case ($\sim 20/15 = 1.33$ nodes per block), our method still outperforms GLM. The possible reason is that the multiple-response GLM approach

does not account for the correlation among the edges, and suffers from overfitting. In contrast, the low-rankness in our modeling incorporates the shared information across entries.

The experiment III compares **STD** with three other supervised tensor methods: Higher-order low-rank regression (**HOLRR**) (Rabusseau and Kadri, 2016), Higher-order partial least square (**HOPLS**) (Zhao et al., 2012) and Subsampled tensor projected gradient (**TPG**) (Yu and Liu, 2016). Figure 3 shows that **STD** outperforms others, especially in the low-signal, high-rank setting. As the number of informative modes (i.e., modes with available features) increases, the **STD** exhibits a substantial reduction in error whereas others remain unchanged (Figure 3b). This showcases the benefit of incorporation of multiple features.

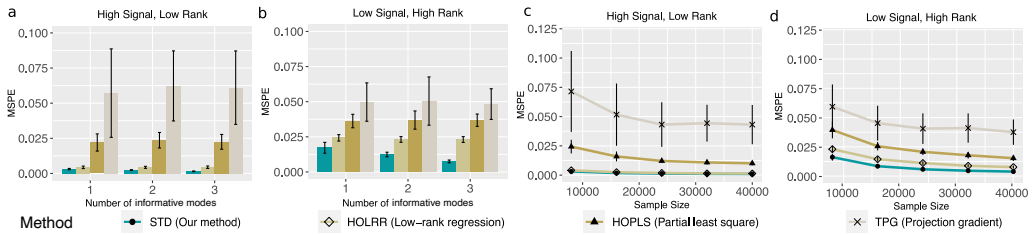

Figure 3: Comparison between different tensor methods. Panels (a) and (b) plot mean squared prediction error (MSPE) versus the number of modes with available features. Panels (c) and (d) plot MSPE versus the effective sample size d^2. We consider rank $\boldsymbol{r} = (3, 3, 3)$ (low) vs (4,5,6) (high), and signal $\alpha = 3$ (low) vs. 6 (high).

We then apply our method to brain structural connectivity networks from Human Connectome Project (HCP) (Geddes, 2016). The dataset consists of 136 brain structural networks, one for each individual. Each brain network is represented as a 68-by-68 binary matrix, where the entries encode the presence or absence of fiber connections between the 68 brain regions. We consider four individual features: gender (65 females vs. 71 males), age 22-25 ($n = 35$), age 26-30 ($n = 58$), and age 31+ ($n = 43$). The goal is to identify the connection edges that are affected by individual features.

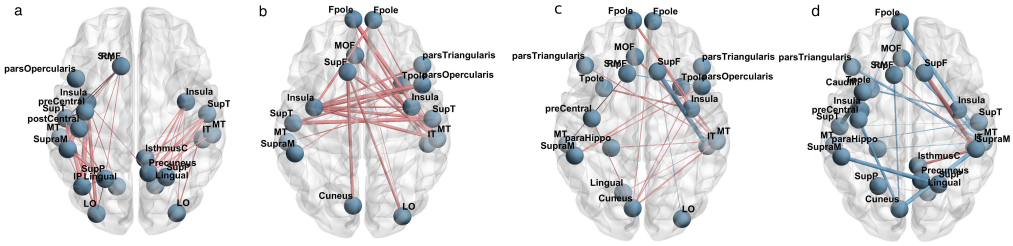

Figure 4: Top edges with large effects. (a) Global effect; (b) Female effect; (c) Age 22-25; (d) Age 31+. Red (blue) edges represent positive (negative) effects. Edge-widths are proportional to the magnitudes of effect sizes.

We appy the supervised tensor decomposition to the HCP data. The BIC selection suggests a rank $\boldsymbol{r} = (10, 10, 4)$ with quasi log-likelihood $\mathcal{L}_{\mathcal{Y}} = -174654.7$. Figure 4 shows the top edges with high effect size, overlaid on the Desikan atlas brain template (Desikan et al., 2006). We find that the global connection exhibits clear spatial separation, and that the nodes within each hemisphere are more densely connected with each other (Figure 4a). In particular, the superior-temproal (*SupT*), middle-temporal (*MT*) and Insula are the top three popular nodes in the network. Interestingly, female brains display higher inter-hemispheric connectivity, especially in the frontal, parental and temporal lobes (Figure 4b). This is in agreement with a recent study showing that female brains are optimized for inter-hemispheric communication (Ingalhalikar et al., 2014). We find several edges with declined connection in the group Age 31+. Those edges involve frontal-pole (*Fploe*), superior-frontal (*SupF*) and cuneus nodes. The frontal-pole region is known for its importance in memory and cognition, and the detected decline further suggests the age effects to brain connections.

5 Conclusion

We have developed a supervised tensor decomposition method with side information on multiple modes. The empirical results demonstrate the improved interpretability and accuracy over previous approaches. Applications to the brain connection data yield conclusions with sensible interpretations, suggesting the practical utility of the proposed approach. Further exploring the benefits of supervised tensor decomposition in specialized tasks will be necessary to boost the scientific discoveries.

Broader Impact

Our supervised tensor decomposition method is widely applicable to network analysis, dyadic data analysis, spatial-temporal model, and recommendation systems. The new method improves the predictive power and enhances interpretability by incorporating of the interactive side information into tensor decomposition. The application to brain connection dataset shows the practical utility of the proposed method. We believe that our model enriches the research of tensor-based learning and becomes a powerful tool to boost scientific discoveries in various fields.

Acknowledgements

The research is supported in part by NSF grant DMS-1915978 and fundings from Wisconsin Alumni Research Foundation. We thank Zhuoyan Xu for the help with the software.

References

Abbe, E. (2017). Community detection and stochastic block models: recent developments. *The Journal of Machine Learning Research*, 18(1):6446–6531.

Berthet, Q. and Baldin, N. (2020). Statistical and computational rates in graph logistic regression. *Proceedings of the Twenty Third International Conference on Artificial Intelligence and Statistics*, 108:2719–2730.

Desikan, R. S., Ségonne, F., Fischl, B., Quinn, B. T., Dickerson, B. C., Blacker, D., Buckner, R. L., Dale, A. M., Maguire, R. P., Hyman, B. T., et al. (2006). An automated labeling system for subdividing the human cerebral cortex on MRI scans into gyral based regions of interest. *Neuroimage*, 31(3):968–980.

Geddes, L. (2016). Human brain mapped in unprecedented detail. *Nature*.

Ingalhalikar, M., Smith, A., Parker, D., Satterthwaite, T. D., Elliott, M. A., Ruparel, K., Hakonarson, H., Gur, R. E., Gur, R. C., and Verma, R. (2014). Sex differences in the structural connectome of the human brain. *Proceedings of the National Academy of Sciences*, 111(2):823–828.

Kolda, T. G. and Bader, B. W. (2009). Tensor decompositions and applications. *SIAM review*, 51(3):455–500.

Lee, C. and Wang, M. (2020). Tensor denoising and completion based on ordinal observations. *International Conference on Machine Learning, to appear, arXiv preprint arXiv:2002.06524*.

Lock, E. F. and Li, G. (2018). Supervised multiway factorization. *Electronic journal of statistics*, 12(1):1150.

Narita, A., Hayashi, K., Tomioka, R., and Kashima, H. (2012). Tensor factorization using auxiliary information. *Data Mining and Knowledge Discovery*, 25(2):298–324.

Rabusseau, G. and Kadri, H. (2016). Low-rank regression with tensor responses. In *Advances in Neural Information Processing Systems*, pages 1867–1875.

Srivastava, M. S., von Rosen, T., and Von Rosen, D. (2008). Models with a kronecker product covariance structure: estimation and testing. *Mathematical Methods of Statistics*, 17(4):357–370.

Wang, M. and Li, L. (2020). Learning from binary multiway data: Probabilistic tensor decomposition and its statistical optimality. *Journal of Machine Learning Research*, 21(154):1–38.

Xu, Z., Hu, J., and Wang, M. (2019). Generalized tensor regression with covariates on multiple modes. *arXiv preprint arXiv:1910.09499*.

Yu, R. and Liu, Y. (2016). Learning from multiway data: Simple and efficient tensor regression. In *International Conference on Machine Learning*, pages 373–381.

Zhao, Q., Caiafa, C. F., Mandic, D. P., Chao, Z. C., Nagasaka, Y., Fujii, N., Zhang, L., and Cichocki, A. (2012). Higher order partial least squares (HOPLS): a generalized multilinear regression method. *IEEE transactions on pattern analysis and machine intelligence*, 35(7):1660–1673.

Zhou, H., Li, L., and Zhu, H. (2013). Tensor regression with applications in neuroimaging data analysis. *Journal of the American Statistical Association*, 108(502):540–552.